Neurobiology of Disease

An Effector-Reduced Anti-β-Amyloid (Aβ) Antibody with Unique Aβ Binding Properties Promotes Neuroprotection and Glial Engulfment of Aβ

Oskar Adolfsson,[1] Maria Pihlgren,[1] Nicolas Toni,[1] Yvan Varisco,[1] Anna Lucia Buccarello,[1] Katia Antoniello,[1] Sophie Lohmann,[1] Kasia Piorkowska,[1] Valerie Gafner,[1] Jasvinder K. Atwal,[2] Janice Maloney,[2] Mark Chen,[2] Alvin Gogineni,[2] Robby M. Weimer,[2] Deborah L. Mortensen,[2] Michel Friesenhahn,[2] Carole Ho,[2] Robert Paul,[2] Andrea Pfeifer,[1] Andreas Muhs,[1] and Ryan J. Watts[2]

[1]AC Immune SA, 1015 Lausanne, Switzerland, and [2]Genentech, South San Francisco, California 94080

Passive immunization against β-amyloid (Aβ) has become an increasingly desirable strategy as a therapeutic treatment for Alzheimer's disease (AD). However, traditional passive immunization approaches carry the risk of Fcγ receptor-mediated overactivation of microglial cells, which may contribute to an inappropriate proinflammatory response leading to vasogenic edema and cerebral microhemorrhage. Here, we describe the generation of a humanized anti-Aβ monoclonal antibody of an IgG4 isotype, known as MABT5102A (MABT). An IgG4 subclass was selected to reduce the risk of Fcγ receptor-mediated overactivation of microglia. MABT bound with high affinity to multiple forms of Aβ, protected against Aβ1–42 oligomer-induced cytotoxicity, and increased uptake of neurotoxic Aβ oligomers by microglia. Furthermore, MABT-mediated amyloid plaque removal was demonstrated using *in vivo* live imaging in hAPP$^{(V717I)}$/PS1 transgenic mice. When compared with a human IgG1 wild-type subclass, containing the same antigen-binding variable domains and with equal binding to Aβ, MABT showed reduced activation of stress-activated p38MAPK (p38 mitogen-activated protein kinase) in microglia and induced less release of the proinflammatory cytokine TNFα. We propose that a humanized IgG4 anti-Aβ antibody that takes advantage of a unique Aβ binding profile, while also possessing reduced effector function, may provide a safer therapeutic alternative for passive immunotherapy for AD. Data from a phase I clinical trial testing MABT is consistent with this hypothesis, showing no signs of vasogenic edema, even in ApoE4 carriers.

Introduction

Alzheimer's disease (AD) is the most common form of neurodegeneration and is exemplified by debilitating dementia. It is proposed that β-amyloid (Aβ) peptides, the proteolytic products of amyloid precursor protein, are toxic and causative in AD, contributing to memory loss and neurodegeneration (Selkoe, 2002). The Aβ1–42 peptide is believed to be the most toxic species, present in various conformational forms (Bitan et al., 2003; Cleary et al., 2005; Shankar et al., 2007). Evidence suggests that some degree of Aβ1–42 oligomerization is necessary for neurotoxicity (Walsh et al., 2002; Kayed et al., 2003; Jan et al., 2011). Furthermore, multiple soluble assembly forms of Aβ1–42 are thought to be both required and sufficient to disrupt neuronal function and subsequent learning and memory (Cleary et al., 2005; Townsend et al., 2006; Poling et al., 2008).

Structural alterations and oligomerization of Aβ1–42 result in a multifaceted dynamic equilibrium of small protofibrillar intermediates in which early oligomeric species act as seeds for fibrillar plaques (Bitan et al., 2003) and thus are of great interest as the primary targets of anti-Aβ therapeutics. A passive anti-Aβ immunotherapy will likely be most beneficial by targeting multiple Aβ1–42 assemblies, including soluble oligomers (Walsh et al., 2005), and other Aβ peptide aggregates that contribute to early events in the Aβ1–42 oligomerization process (Frenkel et al., 1998; Lambert et al., 1998; Lee et al., 2006; Spires-Jones et al., 2009).

An active immunization approach using an Aβ1–42 vaccine was cut short due to safety concerns (Orgogozo et al., 2003), yet some modest long-term functional benefits were reported in antibody responders (Vellas et al., 2009). Active immunization with Aβ carries the risk of adverse immunological responses, leading to inflammation such as meningoencephalitis (Orgogozo et al., 2003), and also lacks the ability to regulate response level and duration. To mitigate these risks, drug development has focused

Received Sept. 15, 2011; revised May 11, 2012; accepted May 17, 2012.

Author contributions: O.A., M.P., N.T., D.L.M., C.H., R.P., A.P., A.M., and R.J.W. designed research; O.A., N.T., Y.V., A.L.B., K.A., S.L., K.P., V.G., J.K.A., J.M., M.C., A.G., R.M.W., D.L.M., M.F., C.H., and R.P. performed research; D.L.M., M.F., A.P., A.M., and R.J.W. contributed unpublished reagents/analytic tools; O.A., M.P., N.T., A.L.B., K.A., K.P., V.G., J.K.A., J.M., M.C., A.G., R.M.W., D.L.M., M.F., C.H., R.P., A.P., A.M., and R.J.W. analyzed data; O.A., M.P., A.M., and R.J.W. wrote the paper.

We thank Yonglian Wu, Kun Peng, Gloria Meng, Jing Li, and Khanh Pham for key insights and data. We thank Bob Kelly for generation of antibody variants. We thank the ABACUS Study Group, including Drs. Adam Boxer, Malgorzata Franczak, Jerome Goldstein, Michael Harris, Melinda Lantz, Jacobo Mintzer, Kyle Patrick, Joel Ross, Beth Safirstein, Franco Sicuro, Louise Taber, Gerald Tramontano, Alexander White, and Donald Royall.

O.A., M.P., N.T., Y.V., A.L.B., K.A., S.L., K.P., V.G., A.P., and A.M. are full-time employees of AC Immune SA. J.K.A., J.M., M.C., A.G., R.M.W., D.L.M., M.F., C.H., R.P., and R.J.W. are full-time employees of Genentech.

Correspondence should be addressed to either of the following: Dr. Ryan J. Watts, Department of Neuroscience, Genentech, 1 DNA Way, South San Francisco, CA 94080, E-mail: rwatts@gene.com; or Dr. Andreas Muhs, AC Immune SA, PSE-EPFL, 1015 Lausanne, Switzerland, E-mail: andreas.muhs@acimmune.com.

DOI:10.1523/JNEUROSCI.4742-11.2012

 0270-6474/12/329677-13$15.00/0

on passive immunization with antibodies targeting Aβ. Although safer, passive immunization may induce antibody–antigen complexes that fully engage Fcγ receptors (FcγRs) on microglia that may provoke adverse proinflammatory reactions, possibly leading to blood–brain barrier (BBB) disruption observed as vasogenic edema and/or cerebral microhemorrhage (Salloway et al., 2009).

Here, we describe a humanized anti-Aβ monoclonal antibody [MABT5102A (MABT)] that targets different Aβ assembly states and contains a human IgG4 backbone with reduced effector function (van der Zee et al., 1986; Tao et al., 1991). MABT effectively reduces Aβ1–42-induced neuronal death and notably promotes microglial Aβ engulfment, but has a significantly reduced capacity to activate microglial FcγRs when compared with an IgG1 subclass.

To directly assess the potential improvement in safety profile, MABT was tested in a single dose, dose-escalation stage, followed by a randomized placebo-controlled, double-blind, parallel multidose (MD) stage phase I clinical study. Patients were also randomized in the MD stage by ApoE status, as previous studies showed that ApoE4 carriers are at higher risk of developing vasogenic edema (Sperling et al., 2012). Consistent with our hypothesis, MABT showed no signs of vasogenic edema at doses as high as 10 mg/kg single dose, or 5 mg/kg MD over four doses. Pharmacokinetic and pharmacodynamic analysis demonstrated a dose-proportional increase in exposure to MABT and a robust elevation in plasma total Aβ levels, which correlated well with serum MABT concentrations, thus confirming that MABT engaged Aβ in humans.

Materials and Methods

Cell culture preparation. Rat primary cortical cultures were prepared from Sprague Dawley rats (Charles River Laboratories) of either sex at postnatal day 1, as described by Meberg and Miller (2003). Cerebellum and meninges were removed, and cortices were cut into small pieces and dissociated with enzymatic disruption at 37°C in dissociation buffer (papain, $CaCl_2$, EDTA, and HEPES; all from Invitrogen). DNase (Invitrogen) was added for 10 min. Following dissociation, dispersed cortical neurons were plated onto poly-L-lysine (0.01%; molecular weight, 150,000–300,000; Sigma-Aldrich)-coated 6-well, 24-well, or 96-well tissue culture plates. For immunocytochemistry, cells were grown on coated glass coverslips, into 24-well plates. Cells were maintained in Neurobasal media (Invitrogen) without phenol red, with the addition of L-glutamine (2 mM; Sigma-Aldrich), B27 supplement (Invitrogen), and penicillin/streptomycin (Sigma-Aldrich) in a humidified incubator at 37°C and 5% CO_2. Following 1 h and 30 min in culture, the medium was replaced with astrocyte-conditioned medium. After further 4 d in culture, cell proliferation was blocked by treatment with cytosine arabinoside at 2.5 μM (Invitrogen). Under these culture conditions, 20% of cells were identified as neurons by NeuN/DAPI staining (data not shown). Experiments using mixed cortical cells were generally performed after culturing cells for 6 d *in vitro*, unless stated otherwise. Enriched microglia prepared from cortex and hippocampus were harvested as described for cortical cultures above. Cortex and hippocampus were put in DMEM containing high glucose and homogenized by pipetting with a 10 ml pipette and then with a syringe. The homogenate was centrifuged for 3 min at 1000 × *g*, and then resuspended in prewarmed DMEM containing high glucose containing 10% FCS and penicillin/streptomycin (microglia media). The cell suspension was next transferred to a T75 tissue-culture flask and kept in a humidified incubator at 37°C and 5% CO_2 for 1 week. The flask was shaken to separate microglia from adherent cells, and collected and washed in DMEM. The resulting cells were resuspended in 1 ml of microglia medium, counted, and plated at 5×10^4 cells/well. To verify microglial enrichment, cells were stained with the astroglial and microglial markers GFAP and Iba1, respectively. Greater than 60% of cells stained positive for Iba1, with no cells staining for both GFAP and Iba1. Pure microglia were prepared from postnatal day 3 CX3CR1-GFP mice (The Jackson Laboratory). Cortex and hippocampus was dissected and triturated in DMEM containing high glucose using a 10 ml pipette, and then with an 18 gauge needle. The homogenate was centrifuged for 3 min at 1000 × *g*, and then resuspended in prewarmed DMEM containing high glucose, 10% FBS, and penicillin/streptomycin (microglia media). The cell suspension was next transferred to a T75 tissue culture flask and kept in a humidified incubator at 37°C and 5% CO_2 for 7–10 d. Microglia were isolated by shaking, collected, and washed in DMEM. The resulting cells were resuspended in 1 ml of microglia medium, counted, and plated on tissue culture-treated glass chamber slides at 5×10^4 cells/well for use in experiments.

Generation of anti-Aβ antibodies and in vivo *efficacy studies.* The disulfide-stabilized IgG4 anti-Aβ monoclonal antibody (mAb) MABT is a humanized form of a mouse IgG2b mAb (mMABT) generated by immunizing mice with a vaccine prepared as previously described (Muhs et al., 2007). For *in vivo* efficacy, both single-transgenic hAPP$^{(V717I)}$ and double-transgenic hAPP$^{(V717I)}$/PS1 female 8- to 9-month-old mice were administered 10 mg/kg purified mMABT once weekly, 2 or 14 times, respectively. Brain Aβ plaque load was evaluated by thioflavin-S staining in the hAPP$^{(V717I)}$ mice, and memory performance by novel object recognition test using the hAPP$^{(V717I)}$/PS1 mice.

Aβ1–42 aggregation assay. Aβ1–42 peptide (Bachem) was dissolved in 1,1,1,3,3,3-hexafluoro-2-propanol, sonicated, and shaken overnight at room temperature. Aliquots were then dried under a flow of argon, vacuum dried, and stored at −80°C as monomeric Aβ1–42 peptide film. For inhibition of aggregation, antibodies were prediluted in PBS and then added to nonsiliconized incubation tubes containing the following: 10 μM thioflavin-T (ThT) (Sigma-Aldrich), 33 μM Aβ1–42 peptide film, and 8.2% DMSO, with a final 10:1 molar ratio of Aβ1–42 to antibody. Incubation was done for 24 h at 37°C, and the spectrofluorescence (excitation, 440 nm; emission, 485 nm) read in six replicates in a black 384-well plate (PerkinElmer) in a microplate reader (Tecan). For disaggregation of preaggregated Aβ1–42, the Aβ1–42 film was made up as a 110 μM solution in 27% DMSO and PBS. This solution was then allowed to aggregate at 37°C for 24 h, after which the following were added: prediluted antibody with a final 10:1 molar ratio of Aβ1–42 to antibody and 10 μM ThT. This solution was then incubated for additional 24 h at 37°C, after which spectrofluorescence was measured as described above. Inhibition of aggregation and disaggregation is expressed as mean percentage (±SEM) inhibition or disaggregation, respectively.

FcγR binding. The binding of test antibodies to a panel of human FcγRs was measured using ELISA. Human FcγRs (Genentech) are fusion proteins containing the extracellular domain of the receptor γ-chain with a Gly/6xHis/glutathione *S*-transferase (GST) polypeptide tag at the C terminus. A mAb with a human IgG1 framework was used as the positive control (IgG1 control) in this experiment. Plates were coated with a mouse monoclonal anti-GST antibody (Genentech) in a 0.05 M sodium carbonate buffer, pH 9.6, overnight at 4°C. After blocking with an assay buffer containing PBS, 0.5% BSA, and 0.05% Tween 20, the plates were incubated with FcγRs at room temperature for 1 h. Human FcγRs were immobilized to the plate via interaction with the anti-GST coating. Serial dilutions of anti-Aβ MABT, MABT-IgG1, MABT-IgG1-D265A, or IgG1 control mAbs were prepared in the assay buffer containing 10% Blocker Casein in PBS (Pierce). Diluted samples were applied as monomeric forms for the high-affinity receptor (FcγRIa), or multimeric forms for the low-affinity receptors (FcγRIIa, FcγRIIb, and FcγRIIIa). The multimeric forms of test antibodies were generated by cross-linking $F(ab')_2$ fragment of goat anti-human κ-chain (MP Biomedicals), with test mAb at an approximate molar ratio of 3:1. The plates were incubated with FcγRs at room temperature for 2 h. Plates were washed three times with wash buffer containing PBS and 0.05% Tween 20 after each incubation step. The antibodies bound to the FcγRs were detected with horseradish peroxidase-conjugated $F(ab')_2$ fragment of goat anti-human $F(ab')_2$ (Jackson ImmunoResearch Laboratories). Tetramethylbenzidine (Kirkegaard & Perry Laboratories) served as a substrate. Plates were incubated at room temperature for 15–20 min to allow color development. The reaction was terminated with 1 M H_3PO_4, and absorbance at 450 nm with reference at 650 nm was measured on a plate reader (Mo-

lecular Devices). Binding curves were generated by plotting the mean absorbance values from duplicates of sample dilutions against the respective sample absorbance.

Preparation of toxic Aβ1–42 oligomers. Aβ1–42 peptide (Bachem) film was prepared as described above. A 165 μg aliquot of peptide film was resuspended in 7 μl of DMSO, 85 μl of PBS, and 9 μl of 2% SDS and incubated for 6 h at 37°C. Then, 300 μl of water was added, and after an overnight incubation at 37°C, Aβ1–42 oligomers were precipitated with 900 μl of 33% methanol 4% acetic acid solution for 1 h at 4°C, centrifuged at 16,200 × *g* for 10 min. Supernatant was removed and Aβ1–42 oligomers were dried before being resuspended in Na_2HPO_4/NaCl solution for a final concentration of 1 μg/μl.

Aβ1–42 cellular toxicity assays. The cytotoxicity of Aβ1–42 oligomers was tested on mixed cortical cultures at day *in vitro* 5 (DIV 5). All antibodies, at a final concentration of 100 μg/ml, were coincubated with Aβ1–42 oligomers for 30 min in serum-free cell culture medium at 37°C before treatment of cells. For some experiments, mixed cortical cultures were pretreated for 1 h with 1 μM *trans*-4-[4-(4-fluorophenyl)-5-(2-methoxy-4-pyrimidinyl)-1*H*-imidazol-1-yl]cyclohexanol (SB239063), a p38MAPK inhibitor, before treatment with Aβ1–42 oligomers. Cell viability was performed by standardized 3-(4,5-dimethylthiazol-2-yl)-2,5-diphenyltetrazolium bromide (MTT) reduction assays (Promega), following the manufacturer's instructions. Briefly, for the last 3 h of treatment, cells grown in 96-well plates (Costar) were incubated with the MTT dye solution and the generation of a blue formazan product was measured by reading absorbance at 570 and 690 nm using a microplate reader (Tecan). Results are presented as a percentage increase in survival over Aβ1–42 oligomer-treated cells. The ability of the MABT mAb to protect neurons from Aβ1–42 oligomer-induced degeneration was also assessed in an *in vitro* assay using immunofluorescence. Embryonic day 17.5 mouse cortical neurons were isolated, dissociated, and cultured *in vitro* in Neurobasal media with B27 supplement. Aβ1–42 was prepared as described above for Aβ1–42 monomeric peptide film, after which 10 μl of DMSO was added to dissolve the peptide. Then, 78.6 μl of Ham's F12 media was added and the Aβ1–42 peptide solution at 25 μM was incubated at 4°C for 48 h before cell treatment. Cells were grown for 9 d in total, and were fed on day 3 and on the day of treatment. For treatment, Aβ1–42 at 2 μM with or without MABT at 50 μg/ml was added at day 5 or day 6, with DMSO-F12 alone at the same volume used for the vehicle control. On day 9, following 3 or 4 d of treatment, neurons were fixed and stained with anti-TuJ1 antibody at 1:1000 dilution. FITC- or Alexa Fluor 488-labeled secondary antibodies were used to visualize $TuJ1^+$ microtubules using fluorescence microscopy.

Immunohistochemistry. Paraffin-mounted temporal lobe brain sections (20 μm) from an AD patient and from an age-matched non-AD control (Tissue Solutions) were used for immunohistochemistry staining. Deparaffinized sections were subjected to antigen retrieval using formic acid and then labeled with 50 μg/ml MABT as the primary antibody. A goat anti-human biotinylated IgG was used as a secondary antibody. Staining was done with diaminobenzidine (Dako) and mounting using Eukitt mounting medium. Images were acquired on a LSM 700 inverted microscope from Zeiss (Carl Zeiss).

Immunocytochemistry and confocal imaging. Cells were grown on glass coverslips. Following treatment, cells were quickly washed with PBS and then fixed with 4% paraformaldehyde for 20 min. After thorough washes, cells were immersed in 100% methanol for 10 min at −20°C. They were then washed again and incubated in a blocking solution, PBS containing 10% normal goat serum for 1 h at room temperature. After an overnight incubation with the primary antibody, cells were washed and incubated for 2 h with the secondary antibody, and then washed and mounted on glass slides using ProLong Gold antifade reagent (Invitrogen). Epifluorescence and confocal images were acquired on a LSM 700 inverted microscope from Zeiss AG, using a 63× lens. Fluorescence intensity was measured in cell bodies delineated by saturated epifluorescence pictures. *Z*-stacks were rendered into a three-dimensional image using ImageJ 1.42 (National Institutes of Health; freeware) from which an apical-to-distal slice containing the labeled proteins was obtained. Cells treated with HyLite Fluor 488-tagged Aβ1–42 were treated in the same way except no primary or secondary antibodies were used to label for Aβ1–42. Pure microglial cultures from CX3CR1-GFP P3 pups were treated with 1 μg/ml lipopolysaccharide (Sigma-Aldrich), 10 μM Aβ1–42 oligomers alone or in combination with 100 μg/ml anti-Aβ MABT, MABT-IgG1, MABT-IgG1-D265A, control IgG1, or antibodies alone for 30 min. Cells were fixed with 4% paraformaldehyde, washed, permeated with cold methanol, blocked with 10% goat serum in PBS, and stained with rabbit anti-phospho-p38MAPK antibody (Cell Signaling Technology).

In vivo *imaging of amyloid plaques.* Cranial windows were implanted above the somatosensory cortex of 10-month-old transgenic $hAPP^{(V717I)}$/PS1 female mice, as previously described (Trachtenberg et al., 2002; Holtmaat et al., 2009), 2 weeks before the initial imaging session. Twenty-four hours before each imaging session, animals were peripherally injected with 10 mg/kg methoxy-X04 intraperitoneally to visualize individual amyloid plaques (Klunk et al., 2002) and immediately before imaging injected intravenously with AngioSense680 (VisEn Medical) to visualize blood vessels. For each imaging session, animals were anesthetized with an isoflurane–oxygen mixture and mounted to the microscope using a head post. Images were collected via a two-photon laser-scanning microscope (Ultima In Vivo Multiphoton Microscopy System; Prairie Technologies) using a Ti:sapphire laser (MaiTai DeepSee Spectra Physics; Newport) tuned to 820 nm delivering ~30 mW to the back-focal plane of a 40×, NA 0.8 objective lens (Olympus Imaging). The pattern of the vasculature was used to reproducibly position the mouse relative to the objective from day-to-day enabling individual amyloid plaques to be imaged over many weeks. The volumes of individual plaques were estimated by summing the number of pixels above background within a region of interest drawn around a given plaque. Background is defined as the mean pixel intensity plus 2 SDs within a region of interest drawn adjacent to an amyloid plaque. Following the fourth and eighth imaging session, animals were dosed intraperitoneally with 60 mg/kg MABT.

Phospho-p38MAPK ELISA. Rat cortical cultures were seeded onto poly-L-lysine-coated six-well cell culture plates (Costar) and used at DIV 5. Unless otherwise indicated, cells were treated with 2 μM Aβ1–42 oligomers with or without mAb at 100 μg/ml for 30 min. In some assays, cells were pretreated for 1 h with the p38MAPK inhibitor SB239063. Anisomycin was used as a positive control. Treatments were stopped by placing cells on ice and aspirating the medium. Cells were washed with ice-cold PBS, harvested using a cell scraper, and lysed in buffer consisting of 50 mM Tris-HCl, pH 8.0, 150 mM NaCl, 5 mM EDTA, 1 mM sodium orthovanadate, 1% Triton X-100, and containing protease and phosphatase inhibitor cocktails. Protein concentration was determined by the BCA assay (Pierce). For semiquantitative measure of p38MAPK activation, a rat phospho-p38MAPK colorimetric ELISA kit was used (Cell Signaling Technology), following manufacturer's instructions. Plates were read on a spectrophotometric microplate reader (Tecan) at a 370 nm.

TNFα release. Rat cortical cultures enriched for microglia (>60% $Iba1^+$ of total $DAPI^+$ cells) were treated with 10 μM Aβ1–42 oligomers with or without 100 μg/ml antibodies for 6 or 24 h. Lipopolysaccharide (Sigma-Aldrich) at 1 μg/ml was used as a positive control stimulus. Cell supernatants were removed at the indicated time points, passed through a 0.2 μm filter, and tested for TNFα with a Quantikine rat TNFα/TNFSF1A (R&D Systems), following the manufacturer's instructions.

Statistical analysis. All statistical analyses were done using GraphPad Prism, version 5 (GraphPad Software). Data are presented as means ± SD or SEM, as indicated. Data were analyzed by Student's *t* test, one-way ANOVA followed by Tukey's *post hoc* multiple comparisons, or Wilcoxon's rank sum nonparametric test when appropriate. A value of $p < 0.05$ was taken to indicate a statistically significant difference.

Results

Generation of a humanized IgG4 antibody, MABT, that binds multiple Aβ conformations

Murine anti-Aβ monoclonal antibodies were generated by immunizing mice with an Aβ peptide antigen using a liposomal vaccine formulation as previously described (Muhs et al., 2007; Hickman et al., 2011). Several criteria were used to select candidate antibodies, including the ability to bind multiple Aβ species

and to inhibit Aβ1–42 assembly into small cytotoxic peptide aggregates. A monoclonal murine mAb with an IgG2b backbone (mMABT) was selected for *in vivo* efficacy studies using both single-transgenic hAPP$^{(V717I)}$ and double-transgenic hAPP$^{(V717I)}$/PS1 female mice. When compared with vehicle control, treatment with mMABT reduced plaque load in mMABT-treated mice by 31%, and improved memory performance with a 32% increase in recognition index as observed in a novel object recognition test (Fig. 1*A*). The mMABT was further affinity matured and humanized onto an IgG4 backbone (referred to as MABT). To test the binding of MABT to Aβ *in vitro*, we made a series of different Aβ1–42 preparations. The binding of MABT was measured by ELISA, and similar to the mMABT (Fig. 1*B*), was shown to be highly comparable among the different Aβ peptides (Fig. 1*C*) or Aβ1–42 assembly states (Fig. 1*D*).

MABT was subsequently tested for binding to Aβ plaques in the brains of transgenic mice expressing the human amyloid precursor protein (hAPP$^{(V717I)}$) and to amyloid plaques in human AD brain sections. Amyloid plaques in both hAPP$^{(V717I)}$ transgenic mice (Fig. 1*E*, top) and in AD brain (Fig. 1*E*, bottom) were immunodecorated with the MABT mAb. Together, these data provide evidence of MABT binding to both soluble Aβ oligomers and Aβ aggregates present in AD brains.

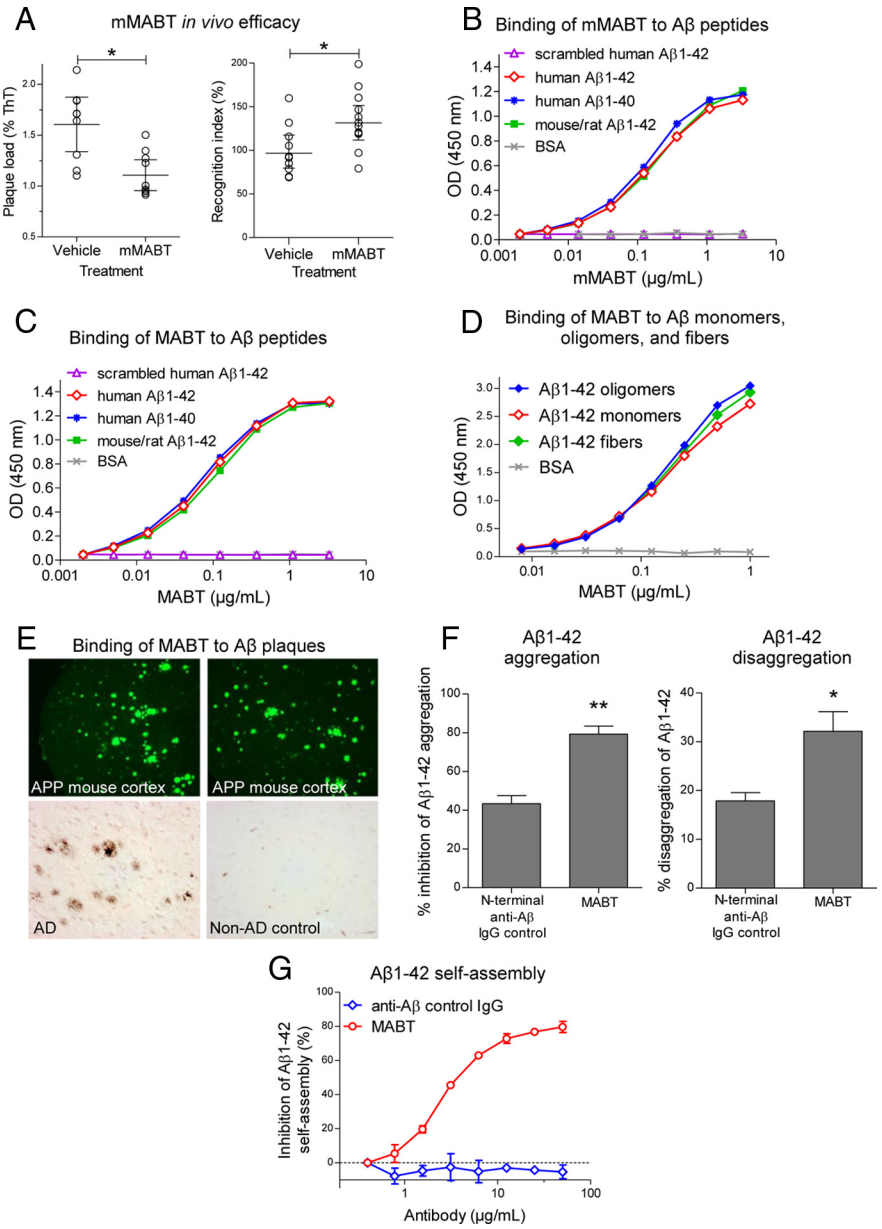

Figure 1. The anti-Aβ MABT mAb binds with high affinity to different Aβ peptides and has antiaggregation properties. ***A***, An *in vivo* efficacy study administering mMABT to hAPP$^{(V717I)}$ mice showed a reduction in Aβ plaque load (left panel) and improved memory performance (right panel). Results show means (±95% CI). ***B***, ***C***, An Aβ ELISA was used to compare the binding to human and murine Aβ1–42 and human Aβ1–40, for mMABT (***B***) and MABT (***C***). ***D***, MABT was also tested for binding to different Aβ1–42 assembly states, showing equal binding for oligomers, monomers, and fibers. ***E***, MABT binds Aβ plaques present in brain sections from transgenic hAPP$^{(V717I)}$ mice (top panels) and human AD temporal neocortical sections (bottom panels). ***F***, *In vitro* functionality was shown by the ability of MABT to impede Aβ1–42 aggregation (left panel), and to disassemble preformed Aβ1–42 aggregates (right panel) in a ThT-based assay, with an Aβ1–42 to MABT molar ratio of 10:1. An anti-Aβ IgG mAb with a N-terminal epitope was used as control. Results show the mean (±SD) of three independent experiments. $*p < 0.05$; $**p < 0.01$. ***G***, MABT was also tested in an Aβ1–42 self-assembly assay that does not rely on ThT fluorescence upon binding to multimeric Aβ assemblies, as described in Materials and Methods. The means (±SEM) of two assays are shown.

Inhibition of Aβ assembly and disaggregation of preformed protofibrillar Aβ peptides by MABT

The binding epitope of MABT was mapped to amino acids 12–23 of Aβ1–42, and therefore overlaps with the main hydrophobic cationic segment of Aβ1–42 responsible for the self-association, subsequent oligomerization, and the core of Aβ1–42 β-sheet assembly (Pike et al., 1993; Esler et al., 1996; Haass and Selkoe, 2007). We therefore hypothesized that MABT would inhibit Aβ1–42 assembly and possibly dissociate preaggregated Aβ1–42. This prompted us to evaluate the effects of MABT on *in vitro* Aβ1–42 aggregation using ThT, a dye that does not impede with amyloid assembly but fluoresces upon binding to amyloid aggregates rich in β-sheets (LeVine, 1993). When we compared MABT to a control anti-Aβ mAb directed against the N terminus of Aβ1–42, and thus not overlapping with the core amino acids that form the self-assembly domain, MABT demonstrated 83% greater inhibitory effect on Aβ1–42 aggregation in a ThT assay (Fig. 1*F*, left panel). Similarly, an 80% greater dissociation of preaggregated Aβ1–42 peptide was observed, when compared with the control N terminus anti-Aβ mAb (Fig. 1*F*, right panel). These *in vitro* assays are based on the ability of ThT to bind to extended β-sheets of the Aβ1–42 peptide (LeVine, 1993). Therefore, to verify that this was not an artifact due to potential mAb-mediated displacement of ThT binding to β-sheet rich Aβ1–42, we performed an assay that does not rely on ThT fluorescence, but rather on the capacity of labeled Aβ1–42 to aggregate or self-assemble onto immobilized unlabeled Aβ1–42. We obtained comparable results in this assay, namely that MABT prevented the self-assembly

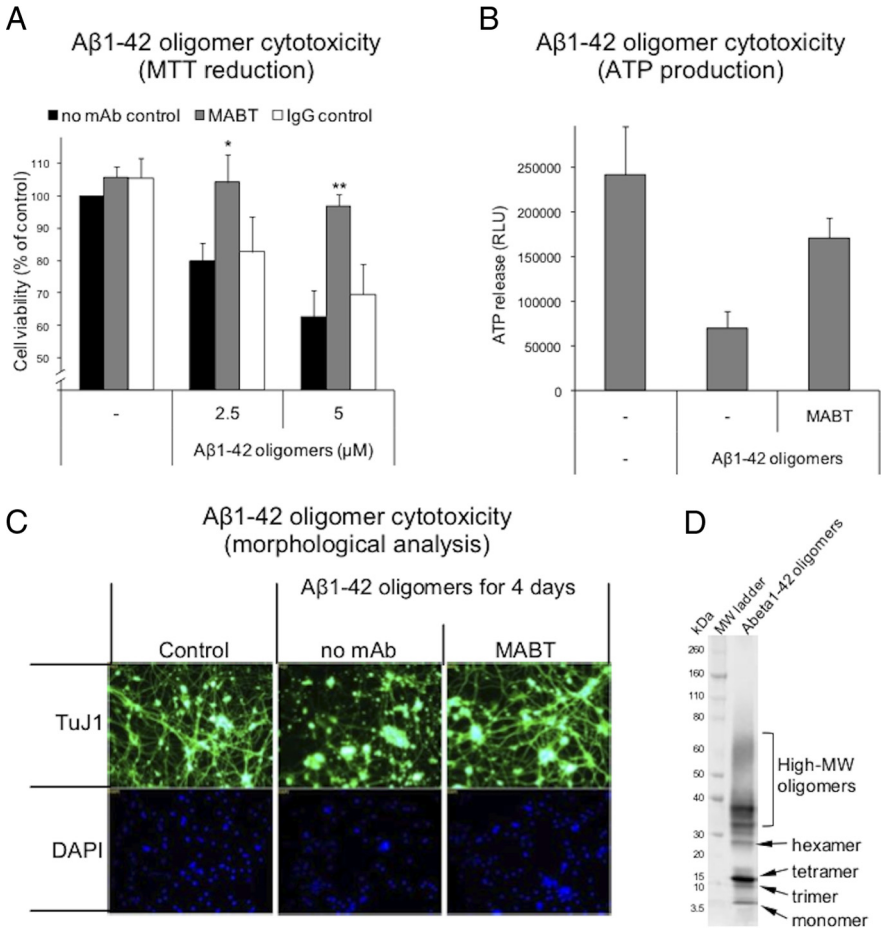

Figure 2. The MABT inhibits cytotoxicity of Aβ1–42 oligomers on primary mixed cortical cultures. ***A***, Mixed cortical cells from P1 rats were treated with 2.5 or 5 μM Aβ1–42 oligomers with or without 100 μg/ml of MABT or an IgG control mAb. An MTT assay was used to determine cell viability as described in Materials and Methods. The means (±SEM) of five independent experiments are shown. $*p < 0.05$; $**p < 0.01$. ***B***, In a comparable assay, but measuring ATP production as a marker of metabolic activity, cells were treated with 10 μM Aβ1–42 oligomers with or without 200 μg/ml MABT. Results show the means (±SEM) of two independent assays. ***C***, Neurotoxicity following extended Aβ1–42 oligomer treatment was tested by morphological analyses. Cells as above were treated for 4 d with 10 μM Aβ1–42 oligomers, with or without 50 μg/ml of MABT, and then stained for TuJ1 (green) and DAPI (blue). ***D***, Silver-stained SDS-PAGE showing the highly cytotoxic Aβ oligomer preparations consisting of a mixture of Aβ1–42 oligomer assemblies, ranging in size from dimers and trimers to higher-molecular-weight multimers.

of Aβ1–42 in a dose-dependent manner (Fig. 1*G*). These data suggest that an antibody directed against the mid-domain of Aβ, yet maintaining binding to aggregated Aβ, may provide the most robust inhibitory effect on Aβ1–42 fibril elongation and/or aggregation relative to antibodies targeting other domains of Aβ.

MABT neutralizes the neurotoxic effects of Aβ oligomers *in vitro*

We next investigated the effects of MABT in a primary cell culture model using cytotoxic Aβ1–42 oligomers. Primary cortical cultures from P1 rats were grown and treated with free Aβ1–42 oligomers or oligomers bound to MABT. Treatment of cortical cultures with 2.5 or 5 μM Aβ1–42 oligomers over 24 h resulted in a reduction in metabolic activity as measured by mitochondrial oxidation of MTT (Fig. 2*A*), an indicator of cell viability. A complete rescue from toxicity was observed for Aβ1–42 oligomer concentration up to 5 μM in the presence of MABT (MABT to Aβ1–42 molar ratio of 1:7.5) compared with control IgG. To confirm these results, ATP release was measured using a luminescence assay, showing a similar neuroprotective effect of MABT (Fig. 2*B*). To further assess the effect of MABT on Aβ1–42-mediated neurodegeneration, mouse embryonic cortical neurons were cultured for 6 d, and treated with Aβ1–42 with or without MABT for 4 d. Control cultures showed healthy morphology (Fig. 2*C*, left panel). Treatment with Aβ1–42 for 4 d resulted in robust neurite degeneration (Fig. 2*C*, center panel). Cells treated with the combination of Aβ1–42 and MABT appeared similar to control cells (Fig. 2*C*, right panel). For these assays, a mixture of cytotoxic Aβ1–42 oligomer assemblies was used, ranging in size from dimers and trimers to higher-molecular-weight multimers (Fig. 2*D*). These results show that MABT was able to protect primary neurons from Aβ1–42 oligomer-induced degeneration.

Aβ1–42 oligomer interaction with neurons is inhibited by MABT

Aβ peptides, especially aggregation intermediates (Bateman et al., 2007), are known to associate with various lipids and proteins present in cell membranes. We hypothesized that MABT may exert its neuroprotective effects by reducing binding of Aβ1–42 oligomers to neurons. To test this idea, an immunofluorescent staining for membrane-bound Aβ was performed. Aβ1–42 oligomers were applied to mixed cortical cultures for 30 min or 18 h, after which cultures were stained for Aβ and the neuron-specific class III β-tubulin, TuJ1. We observed that treatment of cortical neurons with Aβ1–42 oligomers resulted in Aβ binding to neurons, particularly localized to neuritic processes (Fig. 3*A*, middle panels and insets). Cotreatment with MABT blocked the interaction of Aβ1–42 oligomers with neurons. This effect was readily apparent as early as 30 min (Fig. 3*A*,*B*) and remained for at least 18 h of treatment (Fig. 3*B*). Although we used an N-terminal anti-Aβ mAb (clone 6E10) to stain for Aβ1–42 oligomers in our assay (Fig. 3*A*), thus reducing the potential for interference between MABT and the detection mAb used for staining, we confirmed these results using HiLyte Fluor-488 fluorescently labeled Aβ1–42. Treating cortical cultures with this directly labeled Aβ1–42 peptide further supported the conclusion that MABT reduced binding of Aβ1–42 to neuronal processes in primary cortical cultures (Fig. 3*C*,*D*).

Observations from immunofluorescent studies also indicated that, in the presence of MABT, there was a shift in Aβ1–42 oligomer association away from neuronal processes toward cellular profiles that resembled microglia (Fig. 3*E*). This may be expected for an antigen–antibody complex binding to microglia through an FcγR-mediated mechanism (Clark, 1997), but was unexpected for the effector-reduced MABT, which required further investigation.

A role for effector function in microglial uptake of Aβ oligomers

We next explored the relationship between MABT/Aβ1–42 complex formation and microglial uptake of Aβ1–42. To verify that Aβ1–42 oligomers bound to MABT are indeed taken up by microglia, confocal imaging on treated mixed neuronal cultures was performed. When compared with cells treated with Aβ1–42 oligomers alone, we found that MABT mediated rapid uptake of Aβ1–42 oligomers into cellular profiles likely to be microglia (Fig. 4*A*). This was readily apparent as early as 30 min following treatment. Microglia play a crucial role in uptake and degradation of Aβ, a function that is postulated to be compromised in APP transgenic mice (Hickman et al., 2008). Relative to anti-Aβ immunotherapy, it has been proposed that one possible mechanism whereby Aβ plaques are cleared is through the FcγR binding properties of anti-Aβ bound to Aβ (Koenigsknecht-Talboo et al., 2008). However, uptake of anti-Aβ/Aβ complexes by microglia and FcγR activation may trigger these cells to become activated.

In addition to overcoming the direct cytotoxicity of Aβ1–42 oligomers on neurons, a therapeutic anti-Aβ antibody ideally would have a reduced proinflammatory response. We therefore compared MABT to antibodies carrying the same antigen binding sequences, but harboring different IgG backbones with variable FcγR binding affinities, and therefore different microglia activating potential. These included a wild-type human IgG1 with full FcγR binding capacity (MABT-IgG1), and a human IgG1 backbone carrying a D265A mutation (MABT-IgG1-D265A) that dramatically reduces FcγR binding (Shields et al., 2001). All of the backbone variants tested bound with similar affinity to Aβ1–42, as verified using surface plasmon resonance (data not shown). The ability of these different mAb backbones to internalize Aβ1–42 oligomers into microglia was then compared using confocal imaging on Aβ1–42 oligomer-treated primary cortical microglia. We found that Aβ1–42 oligomer internalization correlated well with FcγR binding, with MABT-IgG1 > MABT > MABT-IgG1-D265A (Fig. 4*B*,*C*). To verify that microglia are indeed the cells taking up Aβ1–42 complexed to mAbs, we repeated the study using HiLyte Fluor 488-tagged Aβ1–42 and costained for the microglial marker Iba1. Upon binding to either MABT or MABT-IgG1, tagged Aβ1–42 became enriched in Iba1$^+$ microglia (Fig. 4*D*). We also observed that, in cell cultures treated with Aβ1–42 in combination with MABT-IgG1, microglia had more condensed nuclei and brighter Iba1 staining, features suggesting greater antigen/antibody-mediated microglial activation.

To verify the differences in FcγR binding between MABT backbone variants, we measured the binding of the different cross-linked IgG mAb to FcγRIIIa-V158 and, as expected, found a hierarchy of binding such that MABT-IgG1 > MABT > MABT-IgG1-D265A (Fig. 4*E*). Comparable results were obtained with other members of the FcγR family (data not shown).

We next compared the different MABT variants for their ability to reverse Aβ1–42 oligomer-mediated toxicity in mixed primary cortical cultures. Functional FcγR binding activity, present for both the MABT and MABT-IgG1 mAbs, was required for full reversal of Aβ1–42 oligomer-mediated toxicity (Fig. 4*F*). The MABT-IgG1-D265A mAb, which lacks FcγR binding functionality, showed only a nonsignificant trend toward reversal of Aβ1–42 oligomer-mediated cellular toxicity. Perhaps surprisingly, the MABT-IgG1 wild-type mAb, which bears greater FcγR binding affinity compared with the IgG4 MABT, trended toward a smaller protective effect when compared with MABT. We hypothesized that, while binding to microglial FcγRs is needed for full rescue, the enhanced binding of the MABT-IgG1 backbone to FcγRs compared with that of a MABT may result in undesired microglia activation, which may translate into reduced overall protection against Aβ1–42 oligomer-mediated neurotoxicity.

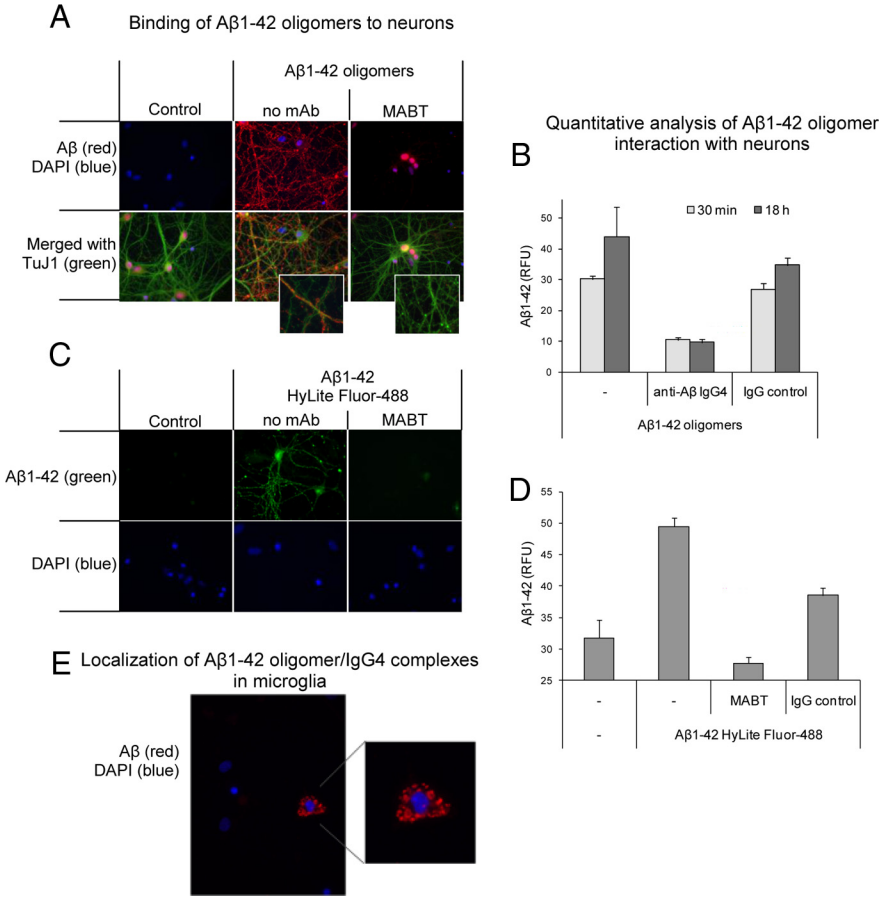

Figure 3. Aβ1–42 oligomer binding to neurites is reduced by the anti-Aβ IgG4 mAb. ***A***, Mixed cortical cells from P1 rats were treated with 2 μM Aβ1–42 oligomers, with or without 100 μg/ml of the MABT or an IgG control for 30 min. The panels from left to right show the following: treatment with buffer control, Aβ1–42 oligomers, and Aβ1–42 oligomers with MABT. Green is TuJ1, red is anti-Aβ (clone 6E10), and blue is DAPI. The bottom row shows all three markers, whereas the top row shows only Aβ and DAPI. The two insets illustrate the binding of Aβ1–42 oligomers to neurites (left) and the inhibition of this binding by the MABT mAb (right). ***B***, Quantitative measures of fluorescence are shown for 30 min and 18 h treatments. Mean results (±SEM) of two experiments are shown. ***C***, Aβ1–42 tagged with HyLite Fluor-488 verifies that MABT inhibits binding of Aβ1–42 to neurites. Cortical cultures from P1 rats were treated as described for ***A***, except that Aβ1–42 tagged with HyLite Fluor 488 was used. Green is Aβ1–42 and blue is DAPI, with one representative experiment shown. ***D***, Green fluorescence was quantified, with the mean (±SD) of the two independent experiments shown. ***E***, Upon treatment with MABT, Aβ1–42 oligomers appeared to be taken up by cells resembling microglia. Green is Aβ1–42 and blue is DAPI.

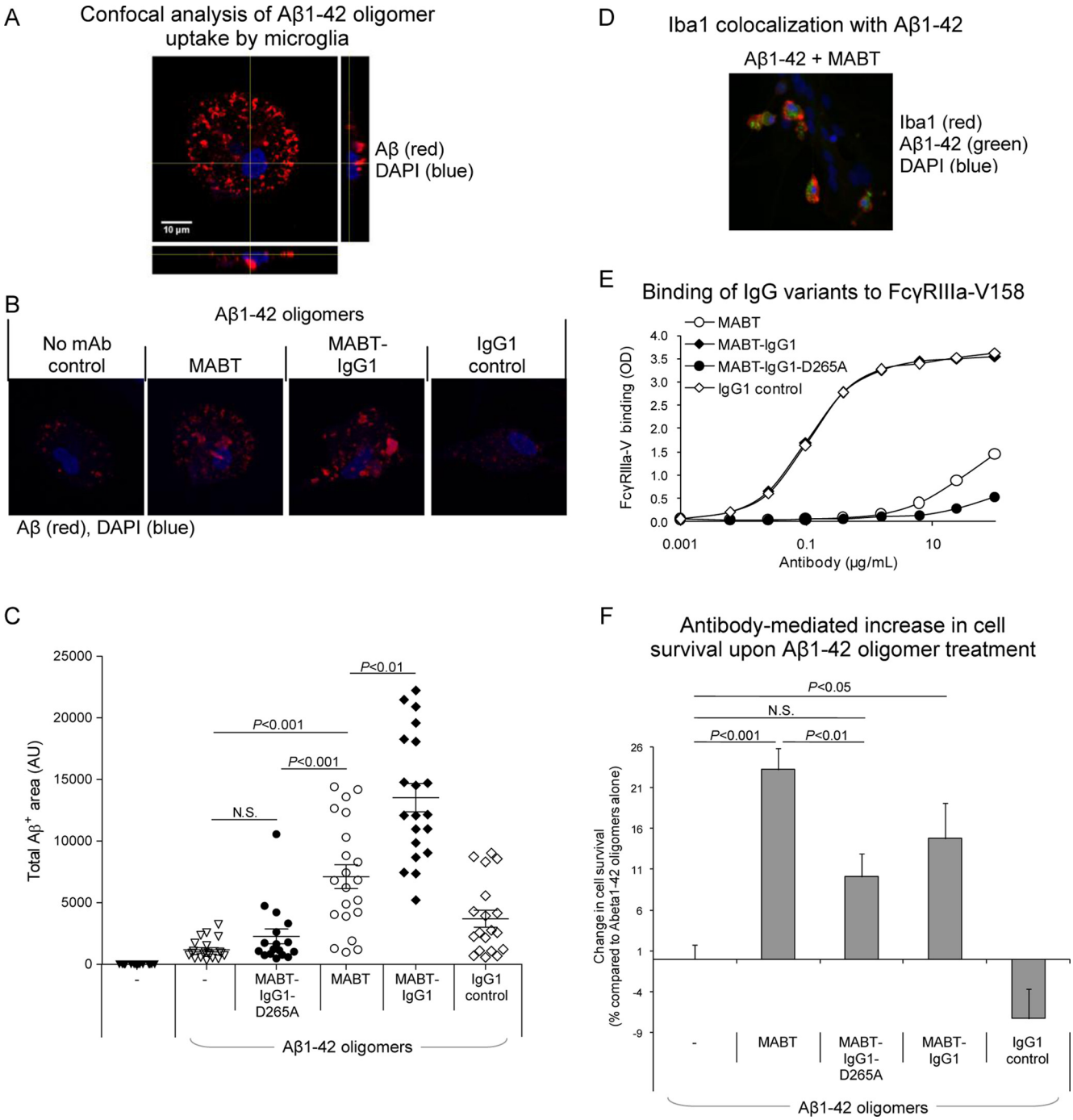

Figure 4. Aβ1–42 oligomers are taken up via an FcR-mediated mechanism into microglia upon MABT treatment. ***A***, Confocal imaging was used to show that Aβ1–42 oligomers complexed to MABT are taken up into microglia. Aβ1–42 oligomers are shown in red, and blue is DAPI. An apical-to-distal slice was obtained from a three-dimensional image rendered from *Z*-stacks. Confocal imaging was done on mixed cortical cells labeled for Aβ (red) and DAPI (blue) as described in Materials and Methods. ***B***, ***C***, Microglia were identified and scanned for the maximum fluorescence intensity through a series of confocal stacks representing intracellular locations (***B***), and the total area of fluorescent signal above a minimum threshold was quantified (***C***). Each mark on the graph represents the total area of Aβ staining within a single cell. A minimum of 20 cells was analyzed for each treatment condition. Data were compared using one-way ANOVA followed by Tukey's *post hoc* multiple comparison. Means (±SEM) are shown. ***D***, Microglia (Iba1^{+}) was verified as the cell type taking up Aβ1–42 complexed to MABT. Red is Iba1, green is HyLite Fluor 488-labeled Aβ1–42, and blue is DAPI. ***E***, Differential binding to FcγRIIIa-V158 was verified in a binding assay. ***F***, An anti-Aβ mAb requires effector function via FcγR binding for full protective effect against Aβ1–42 oligomer toxicity. Mixed cortical cells from P1 rats were treated with Aβ1–42 oligomers, with or without MABT, MABT-IgG1-D265A, MABT-IgG1, or an IgG1 control mAb. The graph shows the mean (±SEM) percentage increase in cell survival compared with Aβ1–42 oligomer treated cells, from five independent experiments. Statistical analysis was done using one-way ANOVA followed by Tukey's *post hoc* multiple comparison.

Therefore, in addition to having the ideal Aβ binding properties, optimizing the level of microglial activation may be crucial in developing an anti-Aβ therapeutic antibody with the desirable safety and efficacy properties.

Having observed that MABT can efficiently promote Aβ engulfment by microglia *in vitro*, we assessed whether systemic administration of MABT in hAPP$^{(V717I)}$ transgenic mice could induce amyloid plaque removal *in vivo*. As the antibodies we

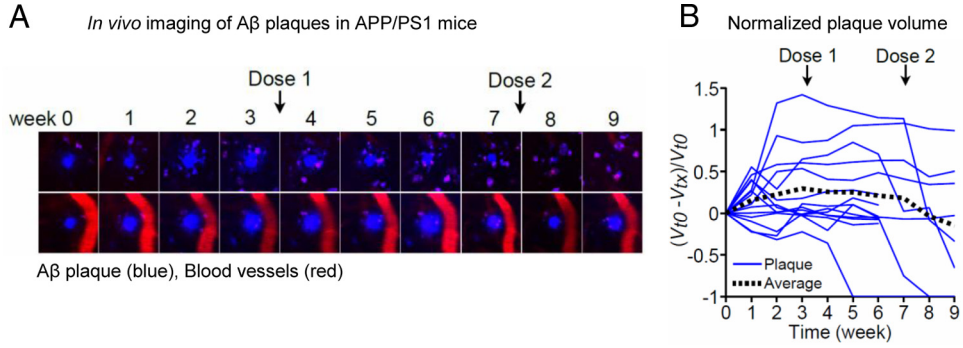

Figure 5. Systemic dosing of MABT modulates individual amyloid plaques *in vivo*. ***A***, Amyloid plaques in hAPP $^{(V717I)}$/PS1 animals were labeled with methoxy-X04 injected intraperitoneally, visualized by *in vivo* two-photon microscopy, and tracked over multiple weeks. ***B***, The relative change in plaque volume over time plotted as fold increase from the initial imaging session. On average, the individual plaque size decreased in volume after systemic dosing with MABT (14 plaques, 2 animals).

generated used human backbones, we were unable to conduct chronic dosing studies as is commonly done for murine antibodies, both because human antibodies can robustly induce an antitherapeutic antibody response and because there is not a murine version of human IgG4 that replicates the Fc receptor binding profile (Fig. 4*E*). Thus, using *in vivo* live-imaging preparations in a short course of dosing, we confirmed the ability of MABT to promote glial engulfment of Aβ by analyzing individual plaques in 10-month-old hAPP $^{(V717I)}$/PS1 transgenic mice over several weeks (Fig. 5*A*). On average, individual plaques increased in volume over the initial 3 week imaging period (Fig. 5*B*, average week-to-week normalized change in volume; 0.156, 0.060, and 0.081). Following a single peripheral MABT administration (60 mg/kg, i.p.), plaque volume decreased over the 3 week period after dosing (average week-to-week normalized change in volume; −0.036, −0.034, and −0.034). A second dose of MABT was administered to a single animal and seven plaques were followed by imaging, three of which were completely removed by week 9. These observations are consistent with our *in vitro* data suggesting that MABT can induce Aβ removal, presumably via microglia uptake.

Reduced microglia response with MABT

To identify downstream mediators of Aβ1–42 oligomer-induced toxicity, we examined a number of candidate signaling pathways. We focused our efforts on examining p38MAPK, which has been shown to contribute to neurotoxicity and microglial activation (Li et al., 2004; Wang et al., 2004). We first examined p38MAPK activation in primary mixed cortical cultures treated with Aβ1–42 oligomers alone, or in combination with the anti-Aβ MABT, MABT-IgG1, MABT-IgG1-D265A, or a control IgG1 that does not bind to Aβ. When cells were treated with Aβ1–42 oligomers, p38MAPK was activated within 15 min (data not shown) and reached a maximum at 30 min. After combining with the different mAbs, only MABT-IgG1, carrying the IgG1 wild-type backbone and thus having the greatest binding affinity to FcγR, significantly increased the Aβ1–42 oligomer-induced p38MAPK activity above Aβ1–42 baseline levels, as shown by a phospho-p38MAPK-specific ELISA (Fig. 6*A*). Since the various anti-Aβ antibodies bind with similar affinity to Aβ1–42, the MABT-IgG1 mAb should neutralize toxic Aβ1–42 oligomers to the same degree as MABT. However, the greater FcγR binding affinity of the IgG1 backbone may result in microglia activation that can be detrimental to cells that are highly susceptible to the actions of Aβ1–42 oligomers, such as neurons. MABT complexed to Aβ1–42 oligomers did not reduce the Aβ1–42 oligomer-induced p38MAPK activity, but rather showed a trend toward higher activity, possibly reflecting the partial FcγR activation by this antibody.

As these initial assays measured the total p38MAPK activity in mixed cortical cultures, including both neuronal and glial cells, we wanted to know whether the p38MAPK activity detected when cells were treated with the combination of Aβ1–42 oligomers and MABT was specific to microglia. Cells were treated as previously, but this time phospho-p38MAPK activity was examined by immunofluorescence staining along with the microglia marker Iba1. Upon treatment with Aβ1–42 oligomers complexed to MABT or MABT-IgG1 mAbs, ~93% of cells staining positive for phospho-p38MAPK were Iba1$^+$ (Fig. 6*B*). To confirm the activation of p38MAPK in microglia, we treated purified microglia in the same way. Under these conditions, Aβ1–42/IgG complex-mediated p38MAPK activation in microglia was readily identified (Fig. 6*C*).

To address the contribution of p38MAPK activation to Aβ1–42 oligomer-mediated neurotoxicity, we next treated cells with a second-generation p38MAPK-specific inhibitor, and then with Aβ1–42 oligomers alone or in combination with either the MABT or the low-FcγR binding MABT-IgG1-D265A mAb. Unexpectedly, the MABT-mediated increase in MTT signal was reduced to that of MABT-IgG1-D265A in presence of the p38MAPK inhibitor, indicating a reduction in MABT-mediated rescue function upon p38MAPK inhibition (Fig. 6*D*). As predicted, p38MAPK inhibition had no effect on cells treated with Aβ1–42 oligomers complexed with the MABT-IgG1-D265A mAb. This indicates that, although the MABT mAb does not significantly induce p38MAPK levels over those seen with Aβ1–42 oligomers alone, p38MAPK activation does play a role in MABT-mediated neuroprotection. The cellular target of this activity in the mixed culture system is not known.

To link the increased microglia activity more directly to a downstream proinflammatory readout, we measured TNFα release by primary cell cultures enriched for microglia (>61% Iba1$^+$; data not shown). The release of proinflammatory TNFα by enriched microglia when treated with Aβ1–42 oligomers was reduced in the presence of all anti-Aβ mAbs tested (Fig. 6*E*). However, the greatest effect was observed in the presence of MABT. Thus, MABT has a more desirable profile compared with MABT-IgG1, combining both the neuroprotective effects with the ability to promote Aβ engulfment by microglia with limited microglial activation. Similar results were observed when evaluating other canonical cytokines; however, these cytokines were not consistently upregulated by the addition of our Aβ oligom-

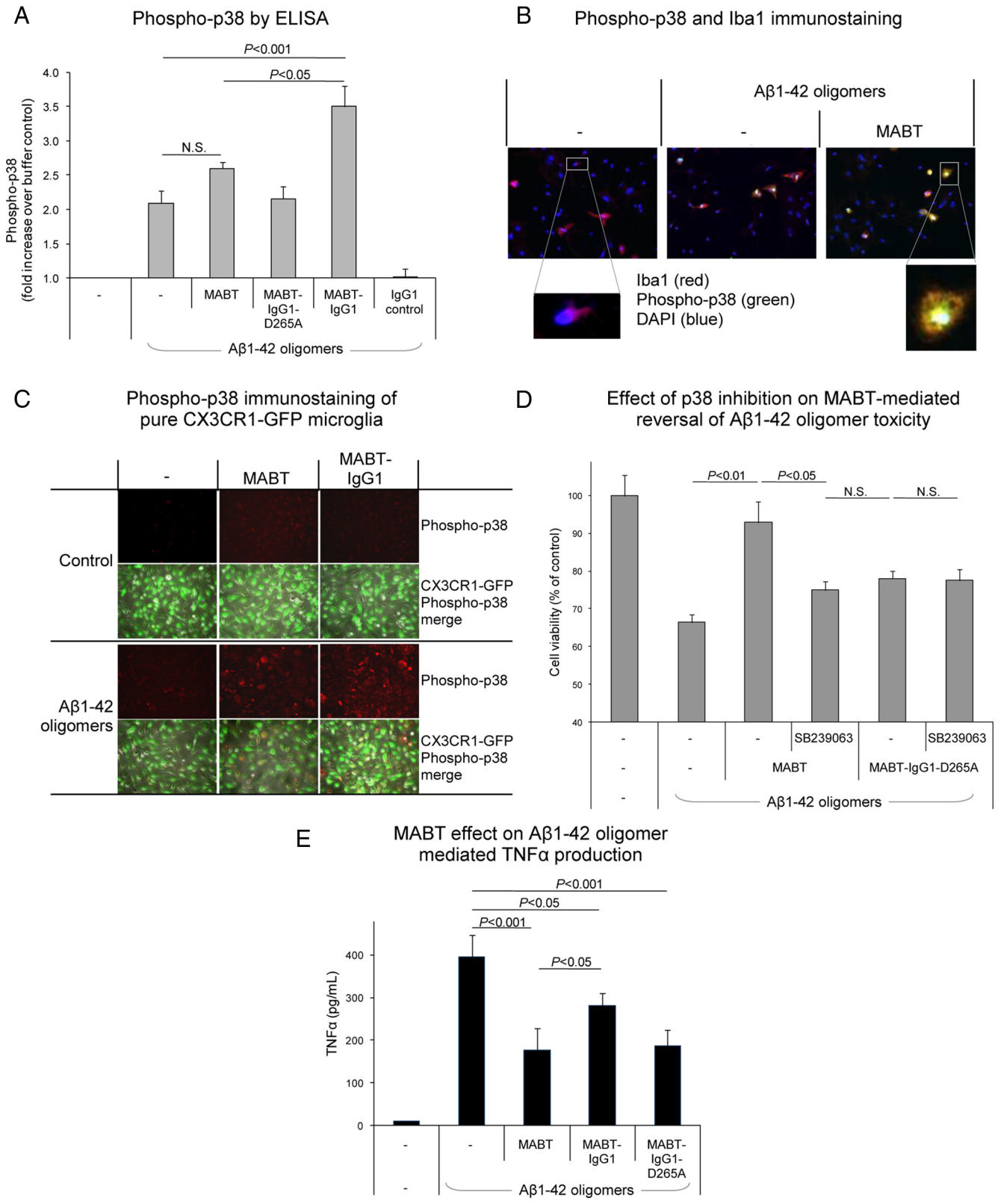

Figure 6. MABT reduces microglial activation as measured by p38MAPK activity and TNFα secretion. ***A***, When complexed to Aβ1–42 oligomers, the IgG1 wild-type backbone significantly increases p38MAPK activation over that shown for Aβ1–42 oligomer-treated microglia. Mixed cortical cells from P1 rats were treated with 10 μM Aβ1–42 oligomers for 30 min with or without 100 μg/ml MABT, MABT-IgG1-D265A, or MABT-IgG1 wild type. An IgG1 mAb not binding to Aβ was used as control. The activity of p38MAPK was measured by a phosphospecific ELISA as described in Materials and Methods. The mean (±SEM) of four independent experiments is shown. Statistical analysis was done using one-way ANOVA followed by Tukey's *post hoc* multiple comparison. ***B***, Activation of p38MAPK with Aβ1–42 oligomers complexed with mAb is specific to microglia. Cells were treated as described above and then stained for phospho-p38MAPK (green), Iba1 (red), and DAPI (blue). The panels from left to right show the following: treatment with buffer control, Aβ1–42 oligomers, and Aβ1–42 oligomers with MABT. ***C***, Pure microglia from CX3CR1-GFP mice were used to verify microglia-specific p38MAPK activity. The top panels show phospho-p38MAPK immunofluorescence (red), whereas the bottom panels are a merge of phospho-p38 and GFP (green) on a phase contrast image. ***D***, p38MAPK activity is required for the full protective effect of MABT against Aβ1–42 oligomer toxicity. Mixed cortical cells from P1 rats were treated (*Figure legend continues.*)

ers; thus, our efforts were focused on evaluating p38MAPK activation and TNFα secretion as consistent measures of microglial activation.

Reduced risk of vasogenic edema with MABT observed in a phase I clinical study

A phase I, randomized, placebo-controlled, double-blind, multicenter clinical study was conducted with the primary objective to determine the safety and tolerability of intravenous MABT in patients with mild-to-moderate AD. Secondary objectives of this study were to characterize pharmacokinetics and Aβ pharmacodynamics after single and multiple doses of MABT in AD patients. The study consisted of a single-dose (SD), dose escalation stage, followed by a randomized placebo-controlled, double-blind, parallel multidose (MD) stage (Fig. 7*A*). The main patient selection criteria included diagnosis of AD (National Institute of Neurological and Communicative Disorders and Stroke and the Alzheimer's Disease and Related Disorders Association criteria), mini-mental state examination score of 15–26 (inclusive) at screening, and a 50–86 years of age range. The actual patient population included in the study are outlined in Figure 7*B*.

No patients receiving MABT developed vasogenic edema, in either the single or multidose study. Importantly, patients were genotyped and randomized in the multidose study to ensure that at least 40% of enrolled patients were ApoE4 carriers (48% were carriers), as these patients were previously shown to be at higher risk of developing vasogenic edema (Salloway et al., 2009). The serum concentration–time profiles for MABT following both a single dose (0.3–10 mg/kg) and four weekly doses (0.5–5 mg/kg) increased in proportion to dose and were characterized by slow clearance ($\sim 3\ ml \cdot d^{-1} \cdot kg^{-1}$) and a long half-life (18–23 d) (Fig. 7*C*). A dose-dependent elevation in plasma total Aβ levels was observed following single or weekly intravenous administration, which correlated well with serum MABT concentrations (Fig. 7*D*), thus suggesting substantial target engagement *in vivo*. These data suggest that an anti-Aβ antibody targeting a wide array of Aβ assembly states, including aggregated Aβ, combined with a human IgG4 backbone with reduced effector function, can be safely dosed in humans at relatively high levels, thus improving CNS exposure. Additional clinical trials are underway to assess the efficacy of MABT (crenezumab).

Discussion

Recent clinical results using both active and passive immunization to target Aβ in AD patients have identified a number of challenges (Orgogozo et al., 2003; Lee et al., 2005; Salloway et al., 2009); thus, great emphasis has been placed on developing alternative strategies toward a safer and more effective immunotherapy for AD. A major theme of the safety findings from these trials, particularly with passive immunotherapy, is disruption of the BBB as observed by magnetic resonance imaging showing signs of vasogenic edema and/or microhemorrhages (Salloway et al., 2009). Mechanisms underlying these dose-limiting observations have been proposed (for review, see Weller et al., 2009). A prominent immunotherapy-specific hypothesis is that the immune functions of the particular anti-Aβ antibody and/or its binding properties are central to the risk associated with these BBB integrity findings (Wilcock et al., 2004, 2006). It has also been hypothesized that these safety findings are inseparable from the mechanisms driving efficacy of immunotherapy (Weller et al., 2009); however, the evidence to support this claim is lacking. For example, previous studies have shown that completely effectorless murine anti-Aβ antibodies are capable of reducing plaque load in mice, while reducing the risks associated with vascular damage (Carty et al., 2006; Wilcock et al., 2006). Nevertheless, these studies did not directly test the ability of these antibodies to promote microglial engulfment of Aβ. Also, these studies were conducted with antibodies that only bind to the less toxic C-terminal region of Aβ1–40. Ideally, an anti-Aβ immunotherapy approach would combine the essential Aβ binding properties to maximize efficacy with the appropriate immune modulation to limit safety findings.

We show that anti-Aβ antibody effector function can be modulated to maintain Aβ engulfment properties, while limiting activation of microglia that may ultimately be deleterious to the vascular and nervous systems. Furthermore, targeting a unique epitope on Aβ has allowed us to identify an antibody that binds multiple forms of Aβ, including oligomeric forms, while inhibiting aggregation and promoting disaggregation of Aβ. Together, the reduced effector function of MABT, a humanized anti-Aβ IgG4 antibody, and its unique Aβ binding profile exclusively position this anti-Aβ immunotherapy candidate to test both mechanisms of efficacy and safety in the clinic. Indeed, phase I data presented in this report are consistent with this hypothesis, showing that, at dose levels and exposure >10-fold compared with other anti-Aβ mAbs on human IgG1 backbones (Salloway et al., 2009; Ostrowitzki et al., 2012), MABT showed no signs of vasogenic edema. Interestingly, however, solanezumab is also on a human IgG1 backbone, but has not shown the same level of vasogenic edema as other human IgG1 anti-Aβ antibodies (Carlson et al., 2011). This is likely because solanezumab does not recognize aggregated Aβ and thus does not bind vascular amyloid and elicit an immune response causing disruption of the blood–brain barrier.

Having identified an anti-Aβ antibody with *in vivo* efficacy and unique binding properties, we set out to investigate the ability of MABT to inhibit Aβ-mediated cellular toxicity. A recent study has demonstrated that the two adjacent histidines at position 13 and 14 of Aβ are necessary for cell membrane binding and uptake (Poduslo et al., 2010). These histidine residues overlap with the epitope of MABT, thus predicting the results of Aβ cellular binding studies in which we observe robust inhibition of Aβ binding to neurons. In addition to blocking Aβ interaction with neurons, we see that toxicity mediated by Aβ oligomers is also inhibited; thus, MABT is neuroprotective to toxicity mediated by Aβ.

In the process of evaluating Aβ-mediated cellular toxicity in mixed neuronal culture systems, which include neurons, microglia, and astrocytes, we observed an accumulation of Aβ after treatment with MABT in an unidentified cell type not resembling a neuron. Further investigation identified this cell type as microglial, based on Iba1 staining and confirmed in studies using purified CX3CR1-GFP microglia. We were intrigued by these initial observations, as MABT is an IgG4 antibody, which has reduced FcγR binding properties compared with a wild-type IgG1 and

←

(*Figure legend continued.*) with 10 μM Aβ1–42 oligomers alone or together with 100 μg/ml MABT or MABT-IgG1-D265A, in the presence or absence of 1 μM SB239063, a p38MAPK-specific inhibitor. A cytotoxicity assay using the MTT readout was performed after 24 h. The mean (±SEM) of four experiments is shown. Statistical analysis was done using one-way ANOVA followed by Tukey's *post hoc* multiple comparison. ***E***, IgG1 is less effective in reducing Aβ1–42-mediated proinflammatory release by microglia as measured by TNFα levels from conditioned media of enriched microglia following 24 h of treatment. The mean (±SEM) of three independent experiments is shown. Statistical analysis was done using one-way ANOVA followed by Tukey's *post hoc* multiple comparison.

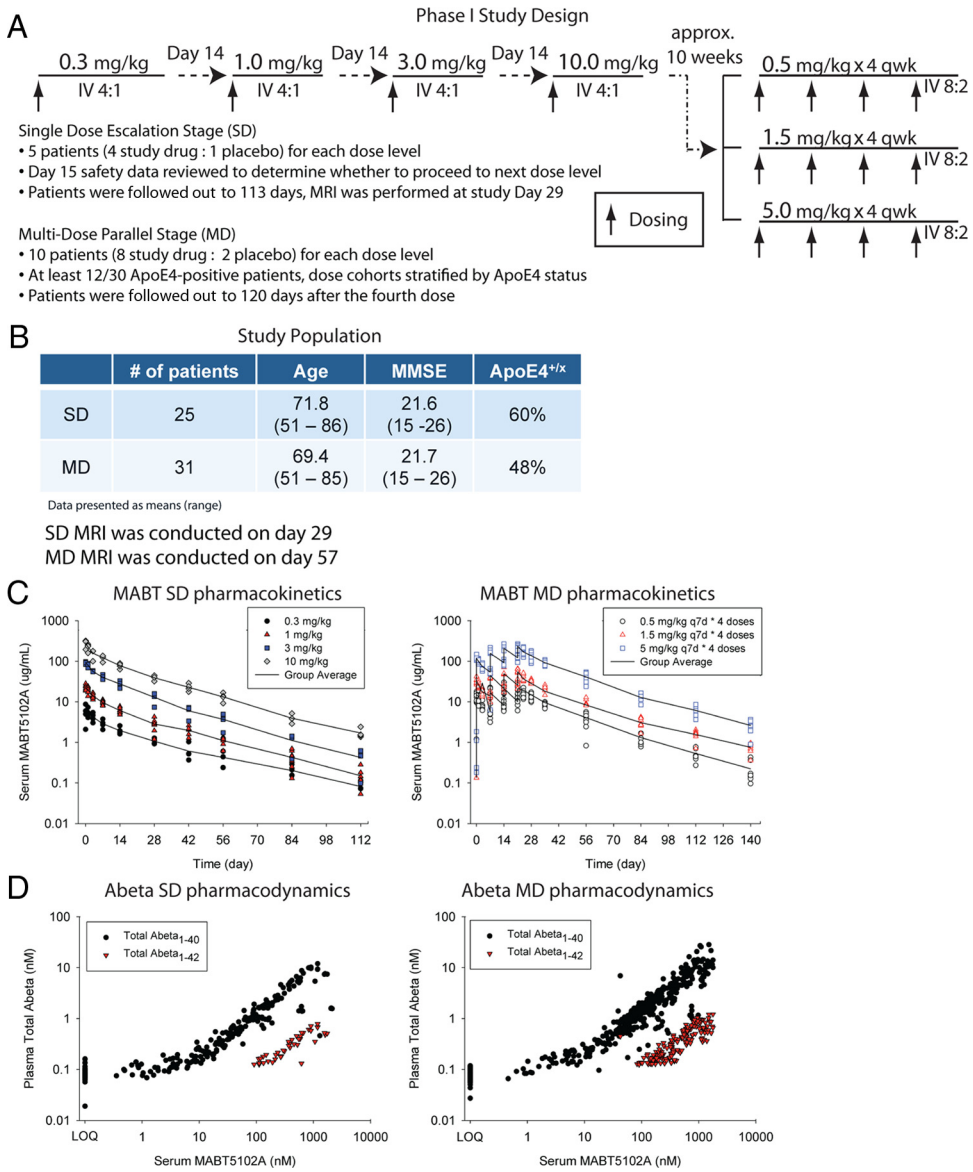

	# of patients	Age	MMSE	ApoE4$^{+/x}$
SD	25	71.8 (51 – 86)	21.6 (15 -26)	60%
MD	31	69.4 (51 – 85)	21.7 (15 – 26)	48%

Figure 7. MABT phase I clinical study results. ***A***, Phase I clinical study design. ***B***, Actual study population. ***C***, The serum MABT concentration–time profiles following both single (SD phase) or weekly (MD phase) intravenous administration increased in proportion to dose and were characterized by slow clearance (~3 ml · d $^{-1}$ · kg $^{-1}$) and a long half-life (18–23 d). ***D***, Increases in plasma total Aβ1–40 and total Aβ1–42 correlated well with serum MABT concentration following single or weekly administration in the SD phase; serum MABT and plasma total Aβ samples were collected just before MABT administration through study day 112. In the MD phase, samples were collected just before MABT administration on day 0, at 1 h and 7 d after each dose and to 119 d after last dose through study day 140. Serum MABT concentrations were determined using a quantitative ELISA with a limit of detection (LOD) of 0.0225 μg/ml. Total plasma levels of Aβ1–40 and Aβ1–42 were determined using an electrochemiluminescence assay with a LOD of 0.01 and 0.125 nM, respectively. Aβ1–42 was not detectable in patients given placebo (or at baseline in patients given MABT) so is not shown.

may therefore be less effective at promoting Aβ engulfment (for review, see Nimmerjahn and Ravetch, 2006). Thus, to explore the relative contribution of IgG isotype and associated effector function to Aβ engulfment by microglia, we generated two additional variants of MABT with equal binding affinity to Aβ, but one with full effector function (MABT-IgG1) and one with no effector function (MABT-IgG1-D265A). Using these reagents, we observed that MABT-IgG4 was nearly as effective as the IgG1 variant at promoting Aβ engulfment. In contrast, MABT-IgG1-D265A showed modest-to-little promotion of Aβ engulfment. These data suggest that effector function may be necessary for Aβ engulfment; however, modest binding to FcγRs may be sufficient to obtain the desired microglial uptake while limiting activation and a proinflammatory response. Furthermore, we confirmed that MABT could reduce Aβ pathology *in vivo* using live imaging in hAPP$^{(V717I)}$/PS1 transgenic mice to assess plaque dynamics after dosing.

Unlike FcγR binding, neonatal Fc receptor (FcRn) binding is not substantially different between IgG4, IgG1, and IgG1-D265A. Although it is notable that altering Fcγ receptor binding alone is sufficient to alter ability of microglial engulfment of Aβ, this does not rule out the possibility that completely effectorless anti-Aβ antibodies may be efficacious *in vivo* via a FcRn-mediated mechanism. Indeed, previous studies have shown that effectorless antibodies are efficacious *in vivo* (Carty et al., 2006; Wilcock et al., 2006); furthermore, an FcRn-driven mechanism of anti-Aβ action has been directly investigated, suggesting that Aβ/anti-Aβ complexes are cleared across the blood–brain barrier via an

FcRn-dependent pathway (Deane et al., 2005). Thus, in addition to the IgG4-dependent ability of MABT to drive microglial engulfment of Aβ, it is also reasonable to propose that MABT could use FcRn to enhance its activity *in vivo*.

Interestingly, MABT-IgG4 and MABT-IgG1 were both neuroprotective; however, the antibody that had no remaining FcγR binding, MABT-IgG1-D265A, was less protective to Aβ-mediated cellular toxicity. Even if full effector function via FcγR binding plays a role in the ability of MABT to promote microglial engulfment of Aβ, MABT-IgG1 did not demonstrate better neuroprotection and may have even shown a trend toward reduced efficacy. We therefore hypothesize that the robust effector function of an anti-Aβ IgG1 antibody, when complexed to Aβ, may aberrantly initiate or augment a proinflammatory response that is detrimental for neuronal cell survival.

There is substantial evidence that microglia are robustly activated in many neurodegenerative diseases, including AD, and that activation may be either neuroprotective or neurotoxic depending on yet poorly understood factors (for review, see Ransohoff and Perry, 2009). The p38MAPK pathway plays a central role in the signaling network responsible for the upregulation of proinflammatory cytokines in microglia, such as TNFα, and regulates their biosynthesis by multiple mechanisms (Simon et al., 1985; J. C. Lee et al., 1994; Gallagher et al., 1997; Y. B. Lee et al., 2000). We therefore assayed for p38MAPK response after Aβ treatment and found that MABT-IgG1 with full effector function produced the greatest activation of p38MAPK in microglia. We also tested for differential effects on TNFα release, a downstream response to p38MAPK activation; all MABT variants tested reduced the release of TNFα by microglia; however, this effect was significantly blunted for MABT-IgG1, which has full effector function. Although there is a well documented role of p38MAPK in stress-induced and proinflammatory signaling, there is also evidence for a supportive function of p38MAPK in Aβ phagocytosis (Doyle et al., 2004) and nonamyloid processing of APP (Bandyopadhyay et al., 2006). These previous findings may explain why the low p38MAPK activity measured from mixed neuronal cultures treated with Aβ and MABT appears to be required for full rescue from toxicity, as the neuroprotective effect of MABT was significantly reduced in the presence of a p38MAPK inhibitor. Considering the entirety of these data comparing various IgG isotypes and subsequent effector function by assaying neuroprotection and microglial activation, we propose that full effector function of an anti-Aβ antibody is not necessary for neuroprotective effects and is likely deleterious when considering enhanced microglial activation as measured by p38MAPK activity and relative TNFα release.

MABT (also known as crenezumab), a humanized anti-Aβ IgG4 effector-reduced antibody, was selected for its *in vitro* and *in vivo* efficacy, including ability to protect neurons from Aβ oligomer-induced toxicity. MABT was also selected for its ability to promote microglial engulfment of Aβ without aberrantly activating microglia. Based on these preclinical data, we hypothesize that MABT would have a reduced risk of vascular-related findings, which are likely a consequence of an anti-Aβ antibody binding aggregated Aβ and maintaining full effector function to elicit a proinflammatory reaction around vascular amyloid. Supported by these preclinical data, a single and multiple dose, multicenter, randomized, placebo-controlled, double-blind phase I study to assess safety, pharmacokinetics, and pharmacodynamics was conducted in patients with mild-to-moderate AD. Magnetic resonance imaging results from this study are consistent with the hypothesis proposed herein, as no patients showed signs of vasogenic edema after either single or multiple doses. Moving forward, larger clinical studies are underway to fully test the efficacy and safety of crenezumab in AD patients.

References

Bandyopadhyay S, Hartley DM, Cahill CM, Lahiri DK, Chattopadhyay N, Rogers JT (2006) Interleukin-1alpha stimulates non-amyloidogenic pathway by alpha-secretase (ADAM-10 and ADAM-17) cleavage of APP in human astrocytic cells involving p38 MAP kinase. J Neurosci Res 84:106–118.

Bateman DA, McLaurin J, Chakrabartty A (2007) Requirement of aggregation propensity of Alzheimer amyloid peptides for neuronal cell surface binding. BMC Neurosci 8:29.

Bitan G, Kirkitadze MD, Lomakin A, Vollers SS, Benedek GB, Teplow DB (2003) Amyloid beta-protein (Abeta) assembly: Abeta 40 and Abeta 42 oligomerize through distinct pathways. Proc Natl Acad Sci U S A 100:330–335.

Carlson C, Estergard W, Oh J, Suhy J, Jack CR Jr, Siemers E, Barakos J (2011) Prevalence of asymptomatic vasogenic edema in pretreatment Alzheimer's disease study cohorts from phase 3 trials of semagacestat and solanezumab. Alzheimers Dement 7:396–401.

Carty NC, Wilcock DM, Rosenthal A, Grimm J, Pons J, Ronan V, Gottschall PE, Gordon MN, Morgan D (2006) Intracranial administration of deglycosylated C-terminal-specific anti-Abeta antibody efficiently clears amyloid plaques without activating microglia in amyloid-depositing transgenic mice. J Neuroinflamm 3:11.

Clark MR (1997) IgG effector mechanisms. Chem Immunol 65:88–110.

Cleary JP, Walsh DM, Hofmeister JJ, Shankar GM, Kuskowski MA, Selkoe DJ, Ashe KH (2005) Natural oligomers of the amyloid-beta protein specifically disrupt cognitive function. Nat Neurosci 8:79–84.

Deane R, Sagare A, Hamm K, Parisi M, LaRue B, Guo H, Wu Z, Holtzman DM, Zlokovic BV (2005) IgG-assisted age-dependent clearance of Alzheimer's amyloid-β peptide by the blood–brain barrier neonatal Fc receptor. J Neurosci 25:11495–11503.

Doyle SE, O'Connell RM, Miranda GA, Vaidya SA, Chow EK, Liu PT, Suzuki S, Suzuki N, Modlin RL, Yeh WC, Lane TF, Cheng G (2004) Toll-like receptors induce a phagocytic gene program through p38. J Exp Med 199:81–90.

Esler WP, Stimson ER, Ghilardi JR, Lu YA, Felix AM, Vinters HV, Mantyh PW, Lee JP, Maggio JE (1996) Point substitution in the central hydrophobic cluster of a human beta-amyloid congener disrupts peptide folding and abolishes plaque competence. Biochemistry 35:13914–13921.

Frenkel D, Balass M, Solomon B (1998) N-terminal EFRH sequence of Alzheimer's beta-amyloid peptide represents the epitope of its anti-aggregating antibodies. J Neuroimmunol 88:85–90.

Gallagher TF, Seibel GL, Kassis S, Laydon JT, Blumenthal MJ, Lee JC, Lee D, Boehm JC, Fier-Thompson SM, Abt JW, Soreson ME, Smietana JM, Hall RF, Garigipati RS, Bender PE, Erhard KF, Krog AJ, Hofmann GA, Sheldrake PL, McDonnell PC, et al. (1997) Regulation of stress-induced cytokine production by pyridinylimidazoles; inhibition of CSBP kinase. Bioorg Med Chem 5:49–64.

Haass C, Selkoe DJ (2007) Soluble protein oligomers in neurodegeneration: lessons from the Alzheimer's amyloid beta-peptide. Nat Rev Mol Cell Biol 8:101–112.

Hickman DT, López-Deber MP, Ndao DM, Silva AB, Nand D, Pihlgren M, Giriens V, Madani R, St-Pierre A, Karastaneva H, Nagel-Steger L, Willbold D, Riesner D, Nicolau C, Baldus M, Pfeifer A, Muhs A (2011) Sequence-independent control of peptide conformation in liposomal vaccines for targeting protein misfolding diseases. J Biol Chem 286:13966–13976.

Hickman SE, Allison EK, El Khoury J (2008) Microglial dysfunction and defective β-amyloid clearance pathways in aging Alzheimer's disease mice. J Neurosci 28:8354–8360.

Holtmaat A, Bonhoeffer T, Chow DK, Chuckowree J, De Paola V, Hofer SB, Hübener M, Keck T, Knott G, Lee WC, Mostany R, Mrsic-Flogel TD, Nedivi E, Portera-Cailliau C, Svoboda K, Trachtenberg JT, Wilbrecht L (2009) Long-term, high-resolution imaging in the mouse neocortex through a chronic cranial window. Nat Protoc 4:1128–1144.

Jan A, Adolfsson O, Allaman I, Buccarello AL, Magistretti PJ, Pfeifer A, Muhs A, Lashuel HA (2011) Abeta42 neurotoxicity is mediated by ongoing nucleated polymerization process rather than by discrete Abeta42 species. J Biol Chem 286:8585–8596.

Kayed R, Head E, Thompson JL, McIntire TM, Milton SC, Cotman CW, Glabe CG (2003) Common structure of soluble amyloid oligomers implies common mechanism of pathogenesis. Science 300:486–489.

Klunk WE, Bacskai BJ, Mathis CA, Kajdasz ST, McLellan ME, Frosch MP, Debnath ML, Holt DP, Wang Y, Hyman BT (2002) Imaging Abeta plaques in living transgenic mice with multiphoton microscopy and methoxy-X04, a systemically administered Congo red derivative. J Neuropathol Exp Neurol 61:797–805.

Koenigsknecht-Talboo J, Meyer-Luehmann M, Parsadanian M, Garcia-Alloza M, Finn MB, Hyman BT, Bacskai BJ, Holtzman DM (2008) Rapid microglial response around amyloid pathology after systemic anti-Aβ antibody administration in PDAPP mice. J Neurosci 28: 14156–14164.

Lambert MP, Barlow AK, Chromy BA, Edwards C, Freed R, Liosatos M, Morgan TE, Rozovsky I, Trommer B, Viola KL, Wals P, Zhang C, Finch CE, Krafft GA, Klein WL (1998) Diffusible, nonfibrillar ligands derived from Abeta1–42 are potent central nervous system neurotoxins. Proc Natl Acad Sci U S A 95:6448–6453.

Lee EB, Leng LZ, Lee VM, Trojanowski JQ (2005) Meningoencephalitis associated with passive immunization of a transgenic murine model of Alzheimer's amyloidosis. FEBS Lett 579:2564–2568.

Lee EB, Leng LZ, Zhang B, Kwong L, Trojanowski JQ, Abel T, Lee VM (2006) Targeting amyloid-beta peptide (Abeta) oligomers by passive immunization with a conformation-selective monoclonal antibody improves learning and memory in Abeta precursor protein (APP) transgenic mice. J Biol Chem 281:4292–4299.

Lee JC, Laydon JT, McDonnell PC, Gallagher TF, Kumar S, Green D, McNulty D, Blumenthal MJ, Heys JR, Landvatter SW (1994) A protein kinase involved in the regulation of inflammatory cytokine biosynthesis. Nature 372:739–746.

Lee YB, Schrader JW, Kim SU (2000) p38 map kinase regulates TNF-alpha production in human astrocytes and microglia by multiple mechanisms. Cytokine 12:874–880.

LeVine H 3rd (1993) Thioflavine T interaction with synthetic Alzheimer's disease beta-amyloid peptides: detection of amyloid aggregation in solution. Protein Sci 2:404–410.

Li R, Yang L, Lindholm K, Konishi Y, Yue X, Hampel H, Zhang D, Shen Y (2004) Tumor necrosis factor death receptor signaling cascade is required for amyloid-β protein-induced neuron death. J Neurosci 24:1760–1771.

Meberg PJ, Miller MW (2003) Culturing hippocampal and cortical neurons. Methods Cell Biol 71:111–127.

Muhs A, Hickman DT, Pihlgren M, Chuard N, Giriens V, Meerschman C, van der Auwera I, van Leuven F, Sugawara M, Weingertner MC, Bechinger B, Greferath R, Kolonko N, Nagel-Steger L, Riesner D, Brady RO, Pfeifer A, Nicolau C (2007) Liposomal vaccines with conformation-specific amyloid peptide antigens define immune response and efficacy in APP transgenic mice. Proc Natl Acad Sci U S A 104:9810–9815.

Nimmerjahn F, Ravetch JV (2006) Fcgamma receptors: old friends and new family members. Immunity 24:19–28.

Orgogozo JM, Gilman S, Dartigues JF, Laurent B, Puel M, Kirby LC, Jouanny P, Dubois B, Eisner L, Flitman S, Michel BF, Boada M, Frank A, Hock C (2003) Subacute meningoencephalitis in a subset of patients with AD after Abeta42 immunization. Neurology 61:46–54.

Ostrowitzki S, Deptula D, Thurfjell L, Barkhof F, Bohrmann B, Brooks DJ, Klunk WE, Ashford E, Yoo K, Xu ZX, Loetscher H, Santarelli L (2012) Mechanism of amyloid removal in patients with Alzheimer disease treated with gantenerumab. Arch Neurol 69:198–207.

Pike CJ, Burdick D, Walencewicz AJ, Glabe CG, Cotman CW (1993) Neurodegeneration induced by β-amyloid peptides *in vitro*: the role of peptide assembly state. J Neurosci 13:1676–1687.

Poduslo JF, Gilles EJ, Ramakrishnan M, Howell KG, Wengenack TM, Curran GL, Kandimalla KK (2010) HH domain of Alzheimer's disease Abeta provides structural basis for neuronal binding in PC12 and mouse cortical/hippocampal neurons. PLoS One 5:e8813.

Poling A, Morgan-Paisley K, Panos JJ, Kim EM, O'Hare E, Cleary JP, Lesné S, Ashe KH, Porritt M, Baker LE (2008) Oligomers of the amyloid-beta protein disrupt working memory: confirmation with two behavioral procedures. Behav Brain Res 193:230–234.

Ransohoff RM, Perry VH (2009) Microglial physiology: unique stimuli, specialized responses. Annu Rev Immunol 27:119–145.

Salloway S, Sperling R, Gilman S, Fox NC, Blennow K, Raskind M, Sabbagh M, Honig LS, Doody R, van Dyck CH, Mulnard R, Barakos J, Gregg KM, Liu E, Lieberburg I, Schenk D, Black R, Grundman M; Bapineuzumab 201 Clinical Trial Investigators (2009) A phase 2 multiple ascending dose trial of bapineuzumab in mild to moderate Alzheimer disease. Neurology 73:2061–2070.

Selkoe DJ (2002) Alzheimer's disease is a synaptic failure. Science 298:789–791.

Shankar GM, Bloodgood BL, Townsend M, Walsh DM, Selkoe DJ, Sabatini BL (2007) Natural oligomers of the Alzheimer amyloid-β protein induce reversible synapse loss by modulating an NMDA-type glutamate receptor-dependent signaling pathway. J Neurosci 27:2866–2875.

Shields RL, Namenuk AK, Hong K, Meng YG, Rae J, Briggs J, Xie D, Lai J, Stadlen A, Li B, Fox JA, Presta LG (2001) High resolution mapping of the binding site on human IgG1 for Fc gamma RI, Fc gamma RII, Fc gamma RIII, and FcRn and design of IgG1 variants with improved binding to the Fc gamma R. J Biol Chem 276:6591–6604.

Simon PL, Laydon JT, Lee JC (1985) A modified assay for interleukin-1 (IL-1). J Immunol Methods 84:85–94.

Sperling R, Salloway S, Brooks DJ, Tampieri D, Barakos J, Fox NC, Raskind M, Sabbagh M, Honig LS, Porsteinsson AP, Lieberburg I, Arrighi HM, Morris KA, Lu Y, Liu E, Gregg KM, Brashear HR, Kinney GG, Black R, Grundman M (2012) Amyloid-related imaging abnormalities in patients with Alzheimer's disease treated with bapineuzumab: a retrospective analysis. Lancet Neurol 11:241–249.

Spires-Jones TL, Mielke ML, Rozkalne A, Meyer-Luehmann M, de Calignon A, Bacskai BJ, Schenk D, Hyman BT (2009) Passive immunotherapy rapidly increases structural plasticity in a mouse model of Alzheimer disease. Neurobiol Dis 33:213–220.

Tao MH, Canfield SM, Morrison SL (1991) The differential ability of human IgG1 and IgG4 to activate complement is determined by the COOH-terminal sequence of the CH2 domain. J Exp Med 173:1025–1028.

Townsend M, Shankar GM, Mehta T, Walsh DM, Selkoe DJ (2006) Effects of secreted oligomers of amyloid beta-protein on hippocampal synaptic plasticity: a potent role for trimers. J Physiol 572:477–492.

Trachtenberg JT, Chen BE, Knott GW, Feng G, Sanes JR, Welker E, Svoboda K (2002) Long-term in vivo imaging of experience-dependent synaptic plasticity in adult cortex. Nature 420:788–794.

van der Zee JS, van Swieten P, Aalberse RC (1986) Inhibition of complement activation by IgG4 antibodies. Clin Exp Immunol 64:415–422.

Vellas B, Black R, Thal LJ, Fox NC, Daniels M, McLennan G, Tompkins C, Leibman C, Pomfret M, Grundman M; AN1792 (QS-21)-251 Study Team (2009) Long-term follow-up of patients immunized with AN1792: reduced functional decline in antibody responders. Curr Alzheimer Res 6:144–151.

Walsh DM, Klyubin I, Fadeeva JV, Cullen WK, Anwyl R, Wolfe MS, Rowan MJ, Selkoe DJ (2002) Naturally secreted oligomers of amyloid beta protein potently inhibit hippocampal long-term potentiation in vivo. Nature 416:535–539.

Walsh DM, Klyubin I, Shankar GM, Townsend M, Fadeeva JV, Betts V, Podlisny MB, Cleary JP, Ashe KH, Rowan MJ, Selkoe DJ (2005) The role of cell-derived oligomers of Abeta in Alzheimer's disease and avenues for therapeutic intervention. Biochem Soc Trans 33:1087–1090.

Wang Q, Walsh DM, Rowan MJ, Selkoe DJ, Anwyl R (2004) Block of long-term potentiation by naturally secreted and synthetic amyloid β-peptide in hippocampal slices is mediated via activation of the kinases c-Jun N-terminal kinase, cyclin-dependent kinase 5, and p38 mitogen-activated protein kinase as well as metabotropic glutamate receptor type 5. J Neurosci 24:3370–3378.

Weller RO, Boche D, Nicoll JA (2009) Microvasculature changes and cerebral amyloid angiopathy in Alzheimer's disease and their potential impact on therapy. Acta Neuropathol 118:87–102.

Wilcock DM, Rojiani A, Rosenthal A, Subbarao S, Freeman MJ, Gordon MN, Morgan D (2004) Passive immunotherapy against Abeta in aged APP-transgenic mice reverses cognitive deficits and depletes parenchymal amyloid deposits in spite of increased vascular amyloid and microhemorrhage. J Neuroinflamm 1:24.

Wilcock DM, Alamed J, Gottschall PE, Grimm J, Rosenthal A, Pons J, Ronan V, Symmonds K, Gordon MN, Morgan D (2006) Deglycosylated anti-amyloid-β antibodies eliminate cognitive deficits and reduce parenchymal amyloid with minimal vascular consequences in aged amyloid precursor protein transgenic mice. J Neurosci 26:5340–5346.